

Characteristics of Acoustic Impulse Response of Submerged Cylindrical Objects as Elements of Target-Scattered Echo

표적신호 시뮬레이션 요소로서 원통형 물수체의 충격응답의 특성

Jae Soo Kim*, Nak Jin Seong**, Sang Young Lee**, Kang Kim**,
Myong Jong Yu**, Woon Hyun Cho**

김재수*, 성낙진**, 이상영**, 김강**, 유명종**, 조운현**

ABSTRACT

Simulation of the target-scattered echo requires the understanding of scattering mechanism at the highlight points. In this paper, the basic assumption of Highlight Model is reviewed through the analyzed data obtained in the acoustic water tank experiment. The analysis shows that the scattering mechanism involves pulse elongation and frequency shift as elements of target-scattered echo, and that the internal structures affect the temporal response of the target-scattered echo significantly. The band-limited impulse response or Green's function due to the diffraction from highlight points of internal structures is not mere delta function, but acts like a filter, which causes frequency shift and is elongated in time.

요약

능동소나에서 표적에 의해 산란된 표적신호를 합성하기 위해서는 반사점(Highlight, 이하 HL)에서의 산란현상의 이해가 선행되어야 한다. 본 논문에서는 음향수조실험에서 얻어진 자료를 분석하여 표적신호를 특징지우고, HL 모델의 기본 가정의 타당성을 검토한다. 수조실험결과는 산란신호가 시간영역에서 신장되고, 도플러효과가 나타나며, 표적의 내부 구조형상이 표적산란신호에 직접반사 이상의 영향을 미침을 보여 준다. 이는 표적산란 신호의 합성에 있어서 사용되는 충격응답 또는 그린 함수(Green's function)가 단순한 델타함수가 아닌 필터역할을 하도록 시뮬레이션해야 함을 보여 준다.

I. Introduction

In order to simulate the target-scattered echo, two kinds of approach are used. One is to model the reflected and diffracted returns from the individual components of the complex structures and to add up these returns coherently [1]. The other

is the Highlight Model which represent the returned signal by source signal convolved with the highlight point distributed over the target [2, 3, 4]. For the development of Sonar system, the highlight model is widely used to represent the temporal and spectral features of echoes scattered by the submerged object in the water.

Highlight Model that consists of a series of separate single delta functions is equivalent to the impulse response of rigid bodies, of which the scat-

*KOREA Maritime University

**ADD

접수일자: 1994년 3월 3일

tering mechanism is well described by Freedman [5, 6]. When the rigid body assumption is relaxed, the details of external geometry as well as internal structures are important making scattering mechanism very complicated, and very few analytic solutions for simple bodies exist. Therefore, from the view point of simulating the target-scattered echo, it is necessary to parameterize and simulate the essential features of the signal since the target echoes vary with detailed structures of the target and behaves like fluctuating target. Such features are pulse elongation, Doppler shift, and strength of the echoes.

The objective of this paper is, therefore, to review the basic assumption of the HL model through the analyzed data obtained in the water tank experiment. This paper consists of four Sections. In Section II, the experimental setup and description of the water tank experiment are introduced, and the essential characteristics of the echoes are discussed. In Section III, in order to analyze the data, the deconvolution techniques in frequency and time domain are discussed. Through deconvolution, impulse response is obtained and interpreted to give insights to simulate the response of the highlight. Also, the method to estimate the optimal time series to simulate the Highlight using deconvolution in time domain is suggested. Finally, summaries are found in section IV.

II. Experimental Setup and Data Interpretations

2.1 Experimental Setup

The experimental setup for acoustic water tank experiment is schematically shown in Fig.1. The dimension of the acoustic water tank is $18 \times 10 \times 10$ (m), whose reflection free time is about 6.6 msec. The target is positioned at the same depth as the projector and receiver. The returns from the insonified length of the target is within the reflection free time, eliminating the interference with the boundary of the water tank. In order to see the change of the echoes due to the internal stru-

cture which is stiffer for this case, two types of target are used, i.e. N-target and S-target (Fig. 2). Two targets are geometrically similar, except that there is a stiffener in S target.

A series of scattering experiment for different aspect angles using CW and FM source signals has been conducted. The definition of aspect angle is shown in Fig.3, and the CW and FM source signals in Fig.4. Since the dimension of target is

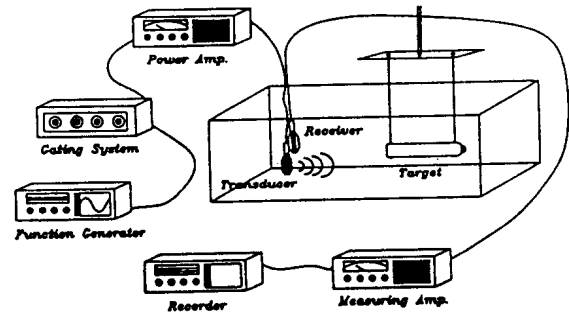
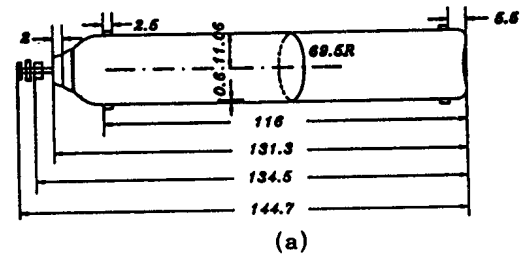
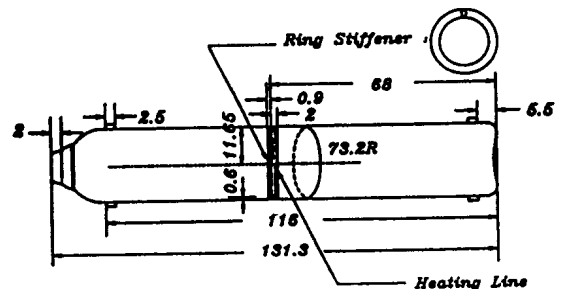


Fig.1 Experimental setup



(a)



(b)

Fig.2 Geometry of the targets (a) without stiffener (b) with stiffener.

131.3 cm and the distance between mono-static hydrophone and target is 300 cm, the projector and receiver is in the near field of target. Therefore, the target strength measurement is not quite meaningful. However, the time series reflects the near-field situation for large target in the close range.

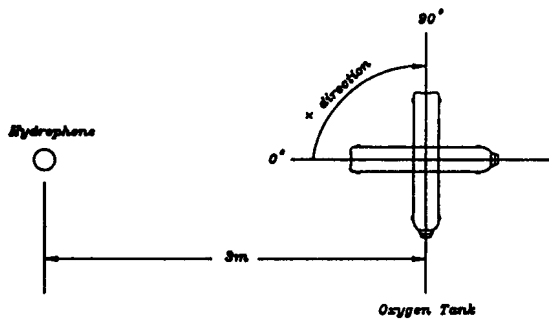


Fig.3 Definition of aspect angle

2.2 Data Interpretations

The types of source signals are used in this experiment, which are CW and FM source signals. The temporal and spectral plots are shown in Fig. 4. The spectral band width of FM source signal is much broader than that of CW source signal.

In Fig.5, the echoes of CW source signal when aspect angle $\theta = 30^\circ$ is shown. The echo for S target shows secondary radiation. The secondary radiation shows significant frequency shift as shown in Fig.6(b) and in Fig.6(c). There are two possible explanations for the observed Doppler shift. One is due to dispersion experienced while the incident wave propagates over the shell. The other is contributed to the directivity of the highlight points, that is, the directivity is dependent on the frequency. Since the exact measurement and the

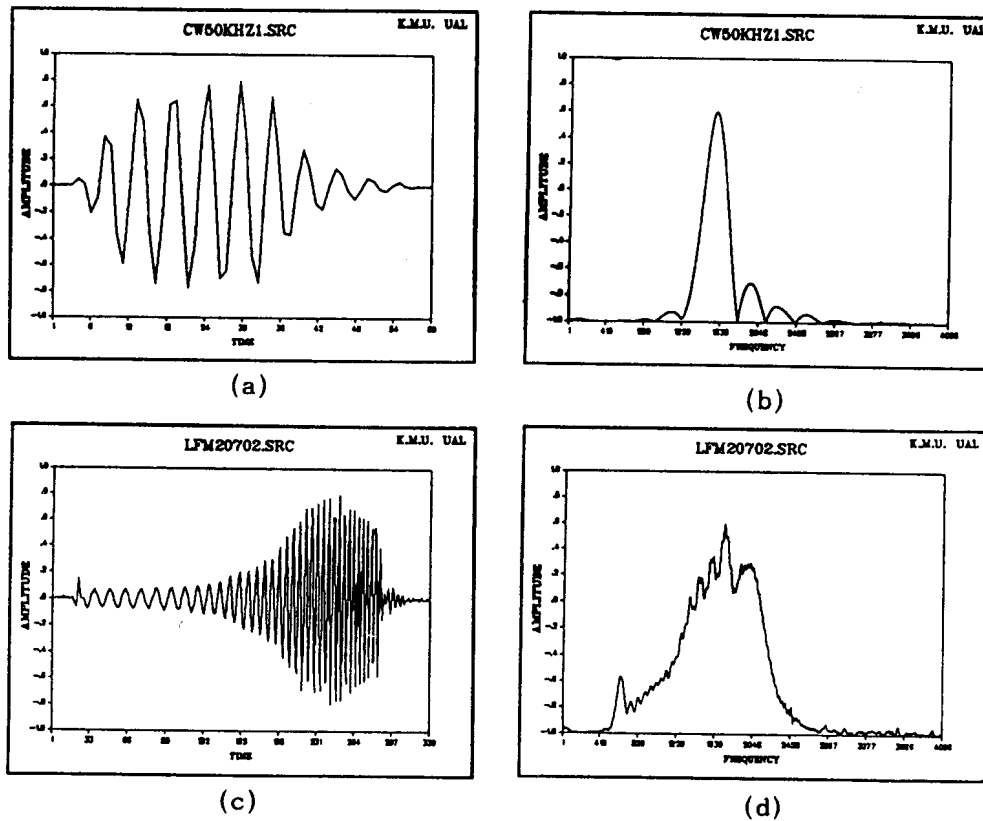


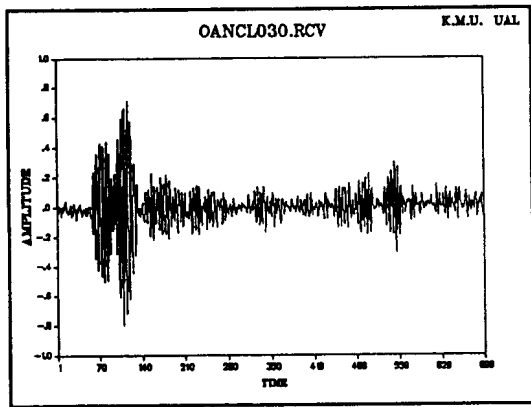
Fig.4 Source signal (a) CW source signal (b) spectrum of CW source signal (c) FM source signal (d) spectrum of FM source signal

exact scattering solution for this geometry do not exist, the complete explanation for the doppler shift is further to be studied.

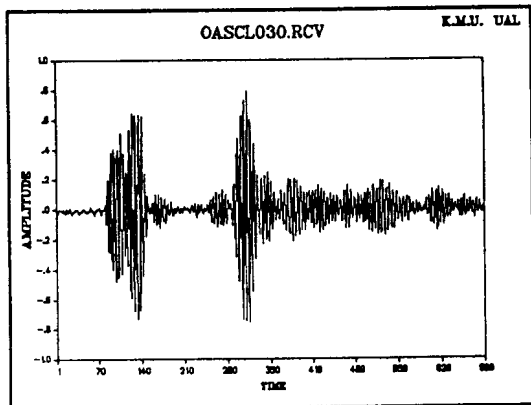
In Fig.7, the echoes for the aspect angle of $\theta = 30^\circ$ is shown. In this figure, the return from the internal structure is even stronger than the returns due to specular reflection. However, this observation might not be general for targets with different proportionality between specular return and secondary radiation.

From the view point of simulating target scattered echo, the data suggest definitively the existence of pulse elongation for different aspect angle when there exist discontinuity of internal

structures, and the frequency shift of the secondary radiation.

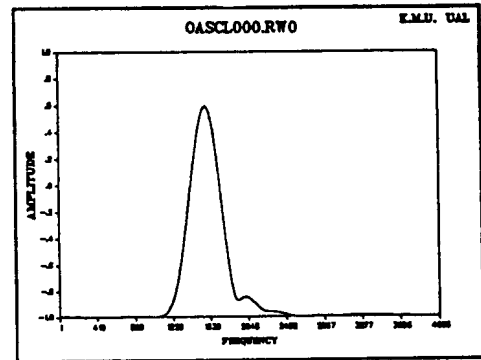


(a)

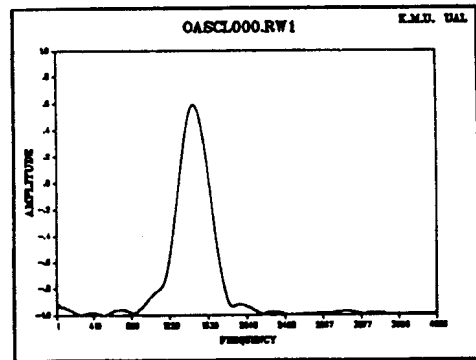


(b)

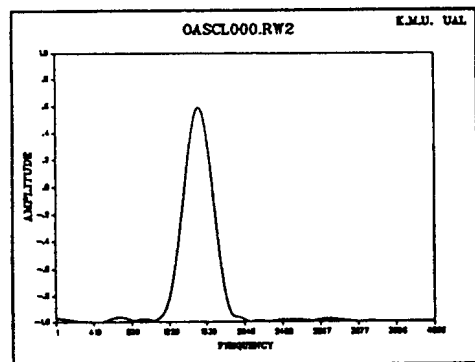
Fig.5 Echoes for CW source signal when aspect angle $\theta = 30^\circ$ (a) N target (b) S target



(a)



(b)



(c)

Fig.6 Spectra of secondary radiation in Fig(5.b) (a) 1st window (b) 2nd window (c) 3rd window

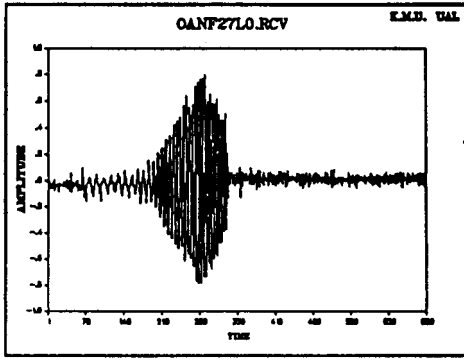


Fig.7 Echoes for FM source signal when aspect angle $\theta = 0^\circ$

III. Acoustic Impulse Response of the Submerged Objects

Deconvolution method is widely used in the system identification of physical system. Some of the examples especially in wave propagation include deconvolving the received signal to find the Green's function (or, band-limited impulse response), where least-squares inversion method is used [7, 8]. Clay used z-transform to estimate the source signature in the bedrock sheet wave guide experiment [9, 10, 11]. As pointed out by Clay [11], the deconvolution by the polynomial division is not stable and vulnerable to the noise contamination.

In this section, the deconvolution methods using FFT and least-square inversion are briefly reviewed and applied to the experimental data. In l_p -deconvolution, $1 \leq p \leq 2$, l_2 corresponds to least-squares inversion. Since it is well known that the least squares inversion is most robust for the experimental data set which might be "inaccurate, insufficient, and inconsistent," according to Lins et. al [12], the least-squares inversion is considered [13].

Throughout the deconvolution experiment, it is assumed that the received signal is obtained from the convolution integral.

$$r(t) = \int_{-\infty}^{+\infty} G(\vec{r}, t; \vec{r}', t-t') s(t') dt' \quad (1)$$

where $G(\vec{r}, t; \vec{r}', t')$ is the Green's function with point source at \vec{r}' with receiver at \vec{r} . The implication of this assumption is that the system response is linear and time-invariant. Since the wave scattering mechanism involves the elements of nonlinear and time-invariant. Since the wave scattering mechanism involves the elements of nonlinear and time-variant characteristics such as dispersion, this assumption is not quite exact to the real world. Nevertheless, the linear approximation is widely used, and we will proceed to the data analysis based on the above assumption.

3.1 Deconvolution Methods

• Deconvolution by FFT

In linear system, the received signal $r(t)$ is expressed as the convolution of source signal $s(t)$ and impulse response $h(t)$, i.e.

$$r(t) = \int_{-\infty}^{+\infty} s(t-\tau) h(\tau) d\tau \quad (2)$$

In frequency domain,

$$R(\omega) = S(\omega) \cdot H(\omega) \quad (3)$$

Therefore, the deconvolution formula in frequency domain is simply

$$H(\omega) = \frac{R(\omega)}{S(\omega)} \quad (4)$$

In the noisy environment, the received signal is expressed as follows

$$R(\omega) = S(\omega) \cdot H(\omega) + N(\omega) \quad (5)$$

When the denominator in Eq(4) gets small, Eq (4) reduces to

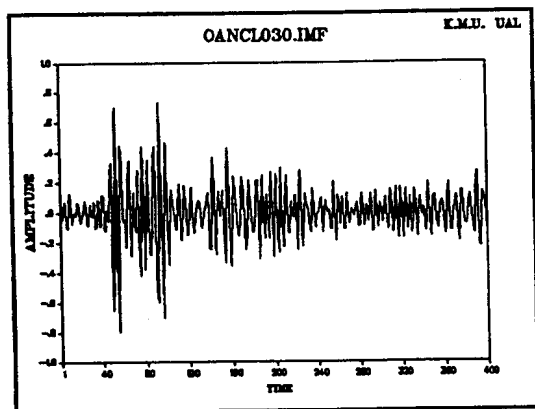
$$H(\omega) \simeq \frac{R(\omega) S^*(\omega)}{|S(\omega)|^2 + |N(\omega)|^2/B^2(\omega)} \quad (7)$$

different spectral characteristics, and accordingly different temporal shape. The impulse response of specular reflection has a well defined peak, while the second and third peaks are more smeared as the arrival time is delayed. This effect is contributed to the propagation effect such as dispersion, that complicates the impulse response.

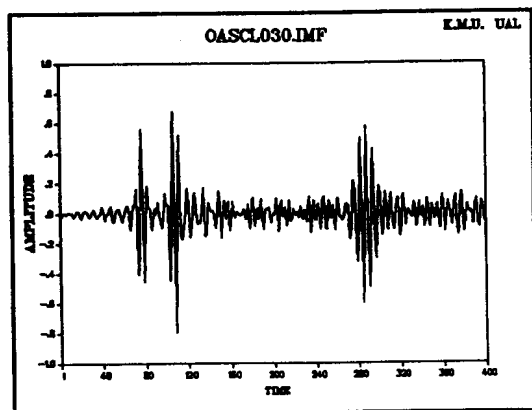
The relatively wide band impulse response of specular reflection using FM pulse (Fig. 4c, 4d) is obtained by deconvolving the received signal (Fig. 7) for the aspect angle of 0° , and shown in Fig. 9. The result suggests that the highlight model is efficient to represent the scattered echo for the

case of specular reflection.

It is noted that the number of highlight points required to simulate the returns due to diffraction at the internal structures increases as the scattering mechanism gets complicated. The optimal shape of the time series for given number of delays to simulate the highlight points can be best determined by least squares inversion. It is equivalent to designing a filter with limited number of time-delay elements.



(a)



(b)

Fig.8 Impulse response when aspect angle $\theta = 30^\circ$ (a) N target (b) S target

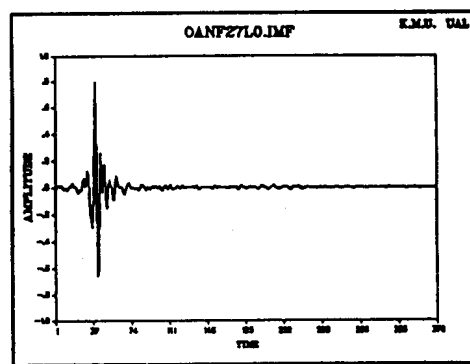


Fig.9 Impulse response when aspect angle $\theta = 0^\circ$

IV. Conclusions

In this paper, the temporal and spectral characteristics of echoes scattered at the HL such as internal structures are examined in view of simulating the target-scattered echo. The experimental data suggest that the target signal is elongated with secondary radiation due to the internal structures. Therefore, the target scattered echo should be modeled as the spread target in space rather than the point target concept. Also, the analyzed data show the scattered signal is not exactly the time-delayed and distributed summation of replica, but show significant doppler shift varying with time. In order to find the impulse response, the experimental data is deconvolved to give band limited impulse response in time domain. The impulse responses show that the High-

light Model can be expanded to accommodate the frequency shift with a series of delta function. However, the nonlinear and time-variant nature of dispersed signal and the relative importance of different type of scattering are to be further understood and simulated. Also, it is noted that the temporal and spectral characteristics of scaled target in the water tank experiment can be significantly modified when applied to the full scale target. Doppler shift observed in the experimental data can be possibly used for the Target State Estimation(TSE) and for discriminating Acoustic Counter Measures(ACM).

References

1. S.I. Hayek, "Acoustic Modeling of the Complex Scatterer," ARL, Penn. State Univ., U.S.A., 1986.
2. S. G. Chamberlain and A. M. Berlinsky, "Coherent Target and Environmental Modeling for Torpedo Terminal Homing Simulation," Electronic Progress, Vol. XXIV, No. 1, Spring, pp. 19-22, Raytheon Company, U.S.A., 1982.
3. D. E. Nelson, A Statistical Scattering Model for Time-Spread Sonar Target, Ph.D. Dissertation, Department of Electrical Eng., Univ. of Rochester, Rochester, New York, U.S.A., 1975.
4. N. J. Seong, J. S. Kim, K. Kim, and S. Y. Lee, "Moving Spread Target Signal Simulation," Journal of Acoustical Soc. of Korea, Vol. 13, No. 2, pp.30-37, 1994.
5. A. Freedman, "A Mechanism of Acoustic Echo Formation," Acustica, 12, 12-21, 1962.
6. A. Freedman, "The High Frequency Echo Structure of Some Simple Body Shapes," Acustica, 12, 61-70, 1962.
7. R. L. Field and J. H. Leclere, "Measurements of Bottom-Limited Ocean Impulse Responses and Comparisons with the Time Domain Parabolic Equation," J. Acoust. Soc. Am. 93, pp.2599-2616, 1993.
8. M. K. Broadhead, R. L. Field, and J. H. Leclere, "Sensitivity of the Deconvolution of Acoustic Transients to Green's Function Mismatch," J. Acoust. Soc. Am. 94(2), Pt. 1, August 1993.
9. C. S. Clay, "Optimum Time Domain Signal Transmission and Source Location in a Waveguide," J. Acoust. Soc. Am. 81(3), March 1987.
10. S. Li and C. S. Clay, "Optimum Time Domain Signal Transmission and Source Location in a Waveguide : Experiments in an Ideal Wedge Waveguide," J. Acoust. Soc. Am. 82(4), October 1987.
11. C. S. Clay and S. Li, "Time Domain Signal Transmission and Source Location in a Waveguide : Matched Filter and Deconvolution Experiments," J. Acoust. Soc. Am. 83(4), April 1988.
12. L. R. Lines and S. Treitel, "Tutorial-A Review of Least-squares Inversion and Its Application to Geophysical Problems," Geophysical Prospecting 32, 159-186, 1984.
13. R. Yarlagadda, J. B. Bednar, and T. L. Watt, "Fast Algorithms for l_p Deconvolution," ASSP, IEEE, Vol. ASSP-33, No. 1, February 1985.
14. W. A. Kuperman, Bottom-Interacting Ocean Acoustics, Plenum Press, New York & London, pp. 193-207, 1980.

- ▲Jae Soo Kim : Vol.13, No.2 참고
- ▲Jea Soo Kim : Vol.13, No.2 참고
- ▲Nak Jin Seong : Vol.13, No.2 참고
- ▲Sang Youn Lee : Vol.13, No.2 참고
- ▲Kang Kim : Vol.13, No.2 참고

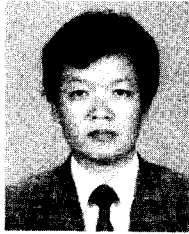
▲Myung Jong Yu



- Educational Experience :
1989. 2 : Kyungpook National University(B.S. in Electronics Eng.)
1991. 2 : Kyungpook National University(M.S. in Electronics Eng.)
- Experience(Military Careers)

Present : Researcher, ADD

▲Woon Hyun Cho



• Educational Experience :

1970 ~ 1974 : Seoul National University (B.S. in Oceanography)

1982 ~ 1985 : Busan National University (M.S. in Geophysics)

1985 ~ 1991 : Texas A & M University (Ph.D. in Geophysics)

• Experience (Military Careers)

1980 ~ 1985 : Researcher, ADD

1991 ~ Present : Senior Researcher, ADD

Chief of Acoustic Detection Division

• 주요 관심분야

Vector wavefield data processing, Wave propagation in anisotropic media, and underwater acoustics

